A regional comparison of particle size distributions and the power law approximation in oceanic and estuarine surface waters

C. J. Buonassissi[1,2] and H. M. Dierssen[1]

Received 11 March 2010; revised 11 June 2010; accepted 21 June 2010; published 13 October 2010.

[1] The particle size distribution (PSD) is commonly used in studies of sediment fluxes, phytoplankton dynamics, and optical scattering from particulates, but little is known about the spatial and temporal variability of this parameter. Here, we analyze in situ laser diffraction measurements of the PSD from a variety of estuarine and open ocean systems. The power law or "Junge-type" distribution provided a good fit to surface ocean particle size distributions measured from 6 to 250 μm. PSD slopes ranged from 2.7 to 4.7 with a mean of 3.63. Consistent with theory, high particle slopes (3.78) and low particle concentrations characterized the open ocean waters of the Atlantic and the Southern Ocean. Lower PSD slopes (3.63) and high concentrations were characteristic of estuarine waters. River plumes consistently showed the lowest PSD slopes (3.30) and highest particle concentrations characteristic of larger bloom-forming phytoplankton and production of particle aggregates. In the North Atlantic, an inverse relationship was found between PSD slope and chlorophyll concentration. Such results follow the biological paradigm that larger phytoplankton are prevalent in bloom conditions and smaller phytoplankton dominate in oligotrophic water. Large temporal variability in PSD was observed in near coastal regions prone to sediment resuspension from storms and tidal flow. Dense sea grass beds consistently had lower particle concentrations compared to surrounding waters due to reductions in current flow and sediment resuspension. Simple power law approximations of particle size distributions can be successfully used to describe and assess particle distributions in a wide array of oceanic and estuarine water types.

Citation: Buonassissi, C. J., and H. M. Dierssen (2010), A regional comparison of particle size distributions and the power law approximation in oceanic and estuarine surface waters, *J. Geophys. Res.*, *115*, C10028, doi:10.1029/2010JC006256.

1. Introduction

[2] The particle size distribution (PSD) represents the relationship between the size of particles and their concentrations in a polydispersion of particles and has been widely used to characterize marine particles [*Bader*, 1970]. Marine PSDs have relevance to diverse fields within oceanography, from biology to sedimentology, and play an important role in climate studies. Assessing the ecological feedbacks to the ocean's carbon cycle requires an understanding of the size of plankton populations [*Chisholm*, 1992; *Falkowski et al.*, 1998]. Size-specific plankton functional types, for example, are being incorporated into global biogeochemical models to better quantify interactions between ocean ecosystems and the climate cycle [*Le Quéré et al.*, 2005]. Additionally, PSD measurements are relevant to the field of sedimentology and have been used to characterize sediment fluxes, resuspension, aggregates, and settling rates in coastal and estuarine waters [*Middleton and Southard*, 1984; *Mikkelsen and Pejrup*, 2001].

[3] The PSD also plays a role in how light scatters in the ocean [*Shifrin and Tonna*, 1993] and directly impacts the oceans optical properties and the water-leaving radiance measured remotely from a satellite. The propagation of light in natural waters depends directly on the cross-sectional scattering area of the particle (related to the size and shape of particle) and the numbers of particles in each size range [*Jonasz and Fournier*, 2007]. The size distribution and refractive index of the particles influences the angular distribution of scattering by oceanic particle assemblages. On the basis of Mie theory [*van de Hulst*, 1981], the PSD can be used with other optical parameters to assess the refractive index of a particle assemblage and the relative contributions of biological and mineralogical components [*Carder et al.*, 1971; *Twardowski et al.*, 2001]. Using a theoretical link between the backscattering spectral slope and the parameters of the power law PSD, PSD has recently been derived globally from ocean color remote sensing imagery with applications to mapping phytoplankton functional groups and their role in carbon sequestration [*Kostadinov et al.*,

[1]Department of Marine Sciences and Department of Geography, University of Connecticut, Groton, Connecticut, USA.
[2]Now at Institute for Coastal Science and Policy, East Carolina University, Greenville, North Carolina, USA.

0148-0227/10/2010JC006256

2009]. While particles in the ocean range from colloids, approximately 1 nm in size, to large organisms many meters long, the relevant size range for bio-optical studies is generally 0.01 μm to 1000 μm encompassing viruses, bacteria, picoplankton, nanoplankton, microplankton, smaller mesozooplankton and sediments [*Jonasz and Fournier*, 2007].

[4] Despite its utility, little is known about natural variability in the PSD due to challenges inherent to its measurement. Some early methods to measure the distribution included shipboard microscopy and screening and filtering to fractionate a sample [*Jonasz*, 1983]. These early techniques were often laborious and time consuming, and produced mixed results. More recent techniques include electrical resistance, flow cytometery, laser diffraction, optical transmission, optical backscatter, and acoustic scattering [*Agrawal and Pottsmith*, 2000; *Jonasz and Fournier*, 2007]. Electrical resistance methods, such as the Coulter counter, pass discrete water samples through orifices of varying size to determine the particle size and count. Such techniques are labor intensive, can aggregate particles, and require the use of multiple orifice tubes to obtain a full PSD. Laser diffraction, the method used here, provides a nondestructive means for measuring in situ particle size distributions in the field over a relatively large size range [*Agrawal and Traykovski*, 2001].

[5] Several mathematical descriptions of the PSD have been used over the years, including power law (or "Junge type"), sum of lognormal functions, Weibull distribution, gamma function, and characteristic vectors (principal components) [*Junge*, 1963; *Bader*, 1970; *Kitchen et al.*, 1975; *Risovic*, 1993; *Jonasz and Fournier*, 1996]. Of these approximations, the power law is the most widely used for optical and ecological purposes [*Jonasz*, 1983; *Briucaud et al.*, 1981; *Stramski and Kiefer*, 1991; *Boss et al.*, 2001; *Twardowski et al.*, 2001]. Many processes and laws in Nature conform to the power law PSD, over many orders of magnitude, such as dust, sea spray, bubble concentrations, sediments [*Monahan and Zietlow*, 1969; *Bader*, 1970] and organismal energetics [*Chisholm*, 1992; *Seibel*, 2007; *Packard and Birchard*, 2008]. While even a cursory examination of PSDs indicates a complexity that cannot be fully captured by a simple approximation, the power law has proven to be a good first-order approximation over several orders of magnitude for oceanic particles.

[6] The PSD slope estimated from the power law model provides information on the relative concentration of small to large particles: the steeper the slope, the greater proportion of smaller particles and the flatter the slope, the greater proportion of larger particles [*Bader*, 1970; *Jackson et al.*, 1997]. For natural waters, PSD slopes generally vary from 3 to 5 with most values between 3.5 and 4 [*Jonasz*, 1983] and can be up to 7 for very small submicron particles [*Loisel et al.*, 2006]. For biooptical applications, the PSD slope is often inferred from the spectral slope of the particulate beam attenuation coefficient [*Boss et al.*, 2001; *Twardowski et al.*, 2001; *Sullivan et al.*, 2005]. However, no such correlation may be evident for water with optically complex assemblages of particles (nonspherical, aggregates, coated particles, etc…) [*Aurin et al.*, 2010].

[7] Even though the power law is commonly used for marine applications, few studies have evaluated the general accuracy and limitations of this approximation for explaining particle distributions in both open ocean, coastal and estuarine ecosystems. *Kitchen* [1977] evaluated several different methods of mathematically describing the particle size distribution for upwelling waters off the Oregon coast and found that some methods like the characteristic vector analysis can be effective, but the hyperbolic (i.e., power law) was more "practical" and proved an equally good fit for particles distributions across the whole size range measured. In contrast, *Stavn and Keen* [2004] compared measurements of suspended minerogenic particle distributions from 40 to 200 μm in the near-coastal ocean to results from a sedimentation model and found that the power law proved inadequate for minerogenic particles in turbid waters.

[8] In this study, the power law approximation is measured across a variety of different marine environments. Laser diffraction from the LISST instrument was used to obtain autonomous, nondestructive, in situ measurements of the particle size distribution across a continuous size spectrum from 6 to 250 μm [*Agrawal and Traykovski*, 2001]. This study is restricted to surface PSD measurements (<5 m) to facilitate comparisons between shallow estuarine and deep water oligotrophic stations and to maximize relevance to remote sensing applications. Analysis of small particles (micron to submicron), while potentially significant for optical scattering [*Stramski and Kiefer*, 1991; *Loisel et al.*, 2006], is beyond the methods employed in this research. By examining particle size distributions in a number of different environments, this study seeks to determine the applicability and limitations of the power law approximation and assess the distributions in a wide variety of natural waters.

2. Methodology

[9] Particle size distributions were collected from 13 different cruises conducted from 2005 to 2009 in a diversity of oligotrophic and estuarine waters from both the east and west coast of the United States and the Atlantic sector of the Southern Ocean. In total, 175 individual stations were sampled. Measurements were taken with a LISST-100X, type B (Laser In Situ Scattering and Transmissometry, Sequoia Scientific) which uses laser diffraction to nominally determine the particle size distribution from 2 to 250 μm with a high sample rate (>1 Hz) [*Agrawal and Pottsmith*, 2000]. Scattered light in the near forward angles is measured on concentric detector rings and inversion modeling based on Mie theory [*van de Hulst*, 1981] yields the volumetric particle concentration in 32 logarithmically spaced size classes. The inversion matrix provided by Sequoia Scientific was used for this study. The volume distribution represents the equivalent volume sphere representation of the true particle assemblage.

[10] The LISST instrument has been successfully used in the marine environment to evaluate suspended floc size and settling rates [*Fugate and Friedrichs*, 2002; *Mikkelsen and Pejrup*, 2001], near-forward optical scattering [*Slade and Boss*, 2006], discriminating complex water types [*Aurin et al.*, 2010], and assessments of phytoplankton assemblages [*Karp-Boss et al.*, 2007; *Anglès et al.*, 2008]. Known inaccuracies with the LISST instruments can result from schlieren in pycnoclines [*Mikkelsen et al.*, 2008] and particles with nonspherical geometry [*Pedocchi and Garcia*,

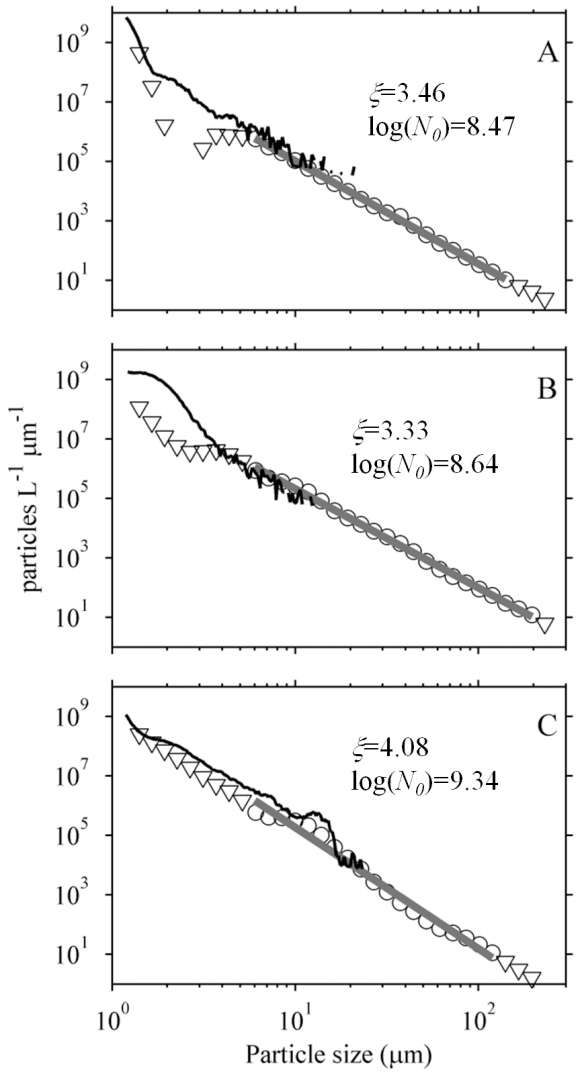

Figure 1. Measured particle concentrations from the LISST (triangles) and the Elzone particle counter (solid black line) for three selected stations within Long Island Sound. Circles and gray line show the size range over which the PSD slope was calculated, excluding points less than 6 μm in size and with concentrations less than 10 particles L^{-1} μm^{-1}.

2006; *Karp-Boss et al.*, 2007; *Agrawal et al.*, 2008]. For comparison purposes, discrete surface water samples from the LIS0505 cruise were also analyzed with an electrical sensing zone method (Elzone particle size analyzer) on the ship within hours after collection.

[11] The power law PSD distribution, $n(D)$, was calculated from the volumetric distribution assuming spherical particles in the assemblage and normalizing by the width of each logarithmically spaced size bin. Analysis was restricted only to measurements of the surface water (<5 m) for each station. A power law approximation was fit to the data

$$n(D) = N_0 D^{-\xi}. \quad (1)$$

The equivalent spherical particle diameter, D, is a nondimensional ratio of the actual particle size to D_0, where D_0 = 1 μm. The nondimensional ξ is the exponent, also referred to as the particle size distribution (PSD) slope. The concentration factor, N_0, is the particle differential number concentration at D (units of particles L^{-1} μm^{-1}, equivalent to 10^9 m^{-4}). The model was fit using the least squares estimator of the log-transformed variables [*Vidondo et al.*, 1997]. Particle concentrations below 10 particles L^{-1} μm^{-1} were considered statistically undersampled and were excluded from the slope calculations.

[12] Field data obtained with the LISST-100X often shows a "tail" at the small end of the size range where the slope is appreciably different from the preceding particle concentrations [*Agrawal et al.*, 2008]. This tail was evident for the majority of stations sampled here and can be produced from assumptions inherent in the scattering matrix used to invert the raw LISST measurements into particle size data. When high concentrations of nonspherical particles or submicron particles (below 2 μm) are present [*Agrawal et al.*, 2008], more laser energy can be diffracted onto the outer rings of the LISST detector than would normally be attributed to spherical particles of 1–2 μm diameter. In addition, ambient red light can be "forward" scattered into the bottom lobe of the outer ring, particularly in near surface waters with sufficient concentrations of red light. The inversion matrix incorrectly identifies this enhanced scattering as high concentrations of particles in the smallest size class and also calculates the contribution of scattering from these imaginary particles into neighboring rings. Because these are not "real" particles that scatter light as anticipated, the inversion can attribute more scattering to these imaginary particles than is available in these neighboring rings. Hence, the retrieved particle size distribution will be high in the smallest size classes and then dip down or even become zero in neighboring larger size classes, producing a PSD with a "tail."

[13] PSD spectra measured in Long Island Sound at three survey stations with the LISST instrument provide examples of this tail visible at size classes less than 6 μm (Figure 1). Coincident particle size distribution measurements taken with the Elzone particle size analyzer for stations from Long Island Sound show no corresponding tail and distributions remain high and roughly log linear throughout the small size classes (Figure 1, black line). The size range sampled with the Elzone instrument spanned a smaller range of particles sizes (1.0 to 24.4 μm) compared to the LISST, but particle concentrations measured over coincident size classes (>6 μm) were found to be generally consistent between the two instruments and provided further confidence in the LISST data over this size range.

[14] Because of inaccuracies at the small size classes, calculation of the LISST PSD slope included only points greater than 6 μm in diameter and with particle counts greater than 10 particles L^{-1} μm^{-1} (Figure 1, circles). The solid gray line shows the fit of the logarithmic regression model used to estimate the PSD slope over the selected size range for three different stations in Long Island Sound. PSD slopes were compared using one-way analysis of variance tests and an R^2 goodness-of-fit test was conducted for each station following *Gaudoin et al.* [2003].

[15] Particle concentrations are presented at a discrete size class (37 μm) throughout the manuscript. At this diameter, the LISST measures volumetric concentrations with a 6 μm

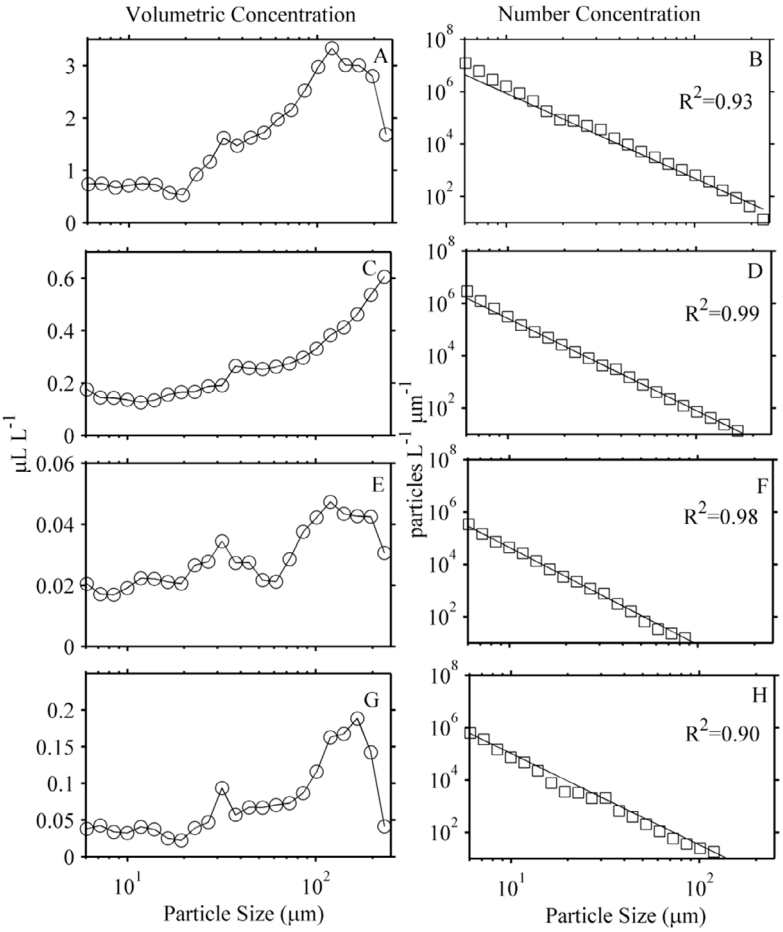

Figure 2. Volumetric concentrations of particles (Figures 2a, 2c, 2e, and 2g) and the corresponding particle number concentrations (Figures 2b, 2d, 2f, and 2h) used in the power law model for (a and b) Hudson River plume during OGCO05, (c and d) St. Joseph Bay 2006, (e and f) Gulf Stream during EDV07, and (g and h) Hudson River plume during OGCO06.

bin size from 34.4 to 40.6 μm. Particle concentrations can be represented as a mean size class based on the integrated particle spectrum, but such values are dependent upon the size spectrum of measured particles. By representing concentrations in a single size class, we wanted to allow for comparisons with data collected from different instrumentation over different particle size ranges. The particle concentration in the 37 μm size class was selected in particular because this diameter is the midpoint in the logarithmic size range and exhibited high variability among stations and regions. However, we note that the concentration at any size class can be estimated from the power law model and PSD slopes following equation (1) and from Table S1 presented in the auxiliary material and by *Buonassissi* [2009].[1]

[16] Chlorophyll *a* (Chl) was determined from filtered discrete surface water samples fluorometrically and measured in triplicate for each station [*Holm-Hansen et al.*, 1965]. Satellite imagery from the Moderate Resolution Imaging Spectroradiometer (MODIS) Aqua sensor for the North Atlantic were downloaded from the National Aeronautics and Space Administration (NASA) ocean color website. Level 3 imagery for Chl and SST (11 μm nighttime), nominally at 9 km resolution, was time averaged over 8 days coinciding with the EDV07 cruise (22–29 March 2007).

3. Results and Discussion

3.1. Applicability of the Power Law Approximation

[17] PSD data are commonly displayed as volumetric concentrations (μL L^{-1}) showing the total volume of particles in each particle size class. Such plots clearly show peaks in selected particle size classes that can be attributed to phytoplankton blooms, larger aggregates, or resuspended sediment (Figure 2). Volumetric concentrations are specific to the width of each size class provided by the instrumentation and must be normalized to the bin width when making comparisons among different types of instruments (μL L^{-1} μm^{-1}). The volume concentrations can also be expressed as the number of equivalent spherical particles per volume at a specific particle diameter, $n(D)$ (particles L^{-1} μm^{-1}). The variability observed in the volumetric distributions is

[1] Auxiliary materials are available in the HTML. doi:10.1029/2010JC006256.

Table 1. Particle Size Distributions of Surface Water < 5 m From Oceanic, Coastal, and Estuarine Waters[a]

Cruise	Location	Subregion	Number of Stations	PSD Slope				Particle Concentration at 37 μm[b]			
				Mean	SD	Min	Max	Median	SD	Min	Max
			Oceanic								
EDV05	North Atlantic	Shelf	7	3.86	0.42	3.18	4.48	61	17	48	95
EDV07	North Atlantic	Shelf	11	3.53	0.74	2.79	4.69	177	135	154	563
	Gulf Stream	Gulf Stream	4	3.84	0.25	3.58	4.19	188	51	161	278
	Sargasso Sea	Sargasso	6	4.06	0.16	3.89	4.31	111	28	88	162
SOGasEx08	Southern Ocean, Atlantic Sector	Patch 1	2	3.94	0.03	3.92	3.97	65	70	16	115
		South Georgia	2	3.90	0.26	3.71	4.08	31	35	7	56
		Patch 2	11	3.70	0.11	3.57	3.92	128	94	44	332
OGCO06	North Atlantic	Shelf	1	3.70	N/A	3.70	3.70	238	N/A	238	238
FBOP05	Florida Shelf	Shelf	2	3.51	0.38	3.24	3.78	460	93	394	526
FBOP06	Florida Shelf	Shelf	2	3.79	0.10	3.72	3.86	175	58	135	216
			Coastal/Estuarine								
EDV07	Narraganssett	Bay	6	3.45	0.14	3.26	3.63	272	71	200	384
MB06	Elkhorn Slough, California	Sea grass/Sediment	4	3.52	0.05	3.48	3.60	4760	2917	3111	9816
FBOP05	Greater Florida Bay	Sand	2	3.68	1.07	2.92	4.44	2470	2693	566	4374
		Sea grass	4	3.28	0.64	2.71	4.03	2288	2149	244	4411
		Mix	2	3.26	0.54	2.87	3.64	2413	2584	586	4240
FBOP06	Greater Florida Bay	Sand	4	4.11	0.10	3.97	4.22	1049	525	788	1914
		Sea grass	8	3.91	0.18	3.60	4.15	274	387	192	1359
		Mix	5	3.91	0.27	3.68	4.35	667	690	250	1921
LISICOS0705	Long Island Sound	Western LIS	23	3.60	0.15	3.26	3.82	2411	1090	1172	5588
LIS0106	Long Island Sound	Eastern LIS	2	3.13	0.16	3.02	3.24	2451	906	1810	3091
LISICOS0306	Long Island Sound	Western LIS	4	3.47	0.04	3.42	3.52	2330	123	2155	2428
LIS0406	Long Island Sound	Western LIS	3	4.06	0.17	3.78	4.1	1613	742	1190	2633
OGCO05	Long Island Sound	Eastern LIS	3	3.79	0.25	3.53	4.05	730	207	583	876
		Central LIS	4	3.95	0.16	3.82	4.13	1406	1035	444	2945
		Western LIS	4	3.92	0.27	3.84	4.41	2140	3678	249	8448
	New York Bight	Shelf	3	3.45	0.26	3.19	3.72	3663	2904	903	6693
OGCO06	Long Island Sound	Western LIS	4	3.82	0.41	3.22	4.10	2258	1322	1071	3906
		Central LIS	3	3.74	0.38	3.34	4.11	1571	511	1083	2105
		Eastern LIS	6	3.50	0.13	3.26	3.63	1402	412	797	2026
	New York Bight	Shelf	3	3.40	0.07	3.32	3.46	1983	872	1172	2907
PSJ06	St. Joseph Bay, Florida	Deep water	2	3.41	0.04	3.38	3.44	2143	383	1872	2414
		Shallow sand	5	3.51	0.07	3.47	3.66	1740	733	1557	3322
			River Plume								
OGCO05	Long Island Sound	Connecticut River	2	2.99	0.35	2.74	3.23	4031	3222	1753	6310
	New York Bight	Hudson River	4	3.21	0.13	3.05	3.35	3673	2364	1167	6864
	New York Bight	Raritan Bay	1	3.62	N/A	3.62	3.62	10,339	N/A	10,339	10,339
OGCO06	Long Island Sound	CT River	3	3.05	0.28	2.74	3.30	5639	1062	4821	6838
	New York Bight	Hudson River	5	3.43	0.04	3.41	3.50	3563	876	2584	4482
	New York Bight	Raritan Bay	1	3.51	N/A	3.51	3.51	4607	N/A	4607	4607
Summary		Oceanic	48	3.78	0.27	2.79	4.66	152	58	47	526
		Estuarine	104	3.63	0.25	2.82	4.41	2062	807	192	9816
		River Plume	16	3.30	0.20	2.74	3.62	4319	1112	1167	10,339

[a]Here SD stands for standard deviation, Min stands for minimum, Max stands for maximum, N/A stands for not available, and LIS stands for Long Island Sound.

[b]Concentrations (particles L^{-1} μm^{-1}) are shown for 37 μm diameter particle, but can be converted to N_o using PSD slope and equation (1). Station-specific data can be found in the auxiliary material and Appendix 1 of *Buonassissi* [2009].

eclipsed when shown as particle concentrations, which closely follow a power law (Figure 2). The log linear fit to the points reveals high regression statistics (Type I), R^2, between 0.90 and 0.99 ($p < 0.01$) for the diverse particle assemblages. For all of the stations sampled, the R^2 for the power law model was >0.87 and all regressions were shown to be significant ($p < 0.01$), indicating that the power law model was generally effective in modeling the PSD. Regression statistics for all of the individual stations are given by *Buonassissi* [2009, Appendix 1].

[18] Several statistical measures were used to evaluate the suitability of the power law approximation. First, an R^2 goodness-of-fit test was conducted for each station following *Gaudoin et al.* [2003]. Linear regression was performed between the log-transformed measured particle concentration and the predicted values using the power law regression slope and intercept for each station. The goodness of fit was evaluated by the magnitude of R^2 and the similarity of the calculated regression slope and intercept to 1 and 0, respectively, indicating perfect agreement between measured and modeled distributions. For the goodness of fit regressions, a regression intercept of 0 and a regression slope of 1 fell within the 95% confidence interval for 97% and 91% of all stations, respectively. All regressions were significant ($p < 0.01$). The median regression slope for all stations was 0.98 and intercept of 0.05, indicating that the modeled relationship adequately followed the entire particle size range for a majority of the stations (Table 1).

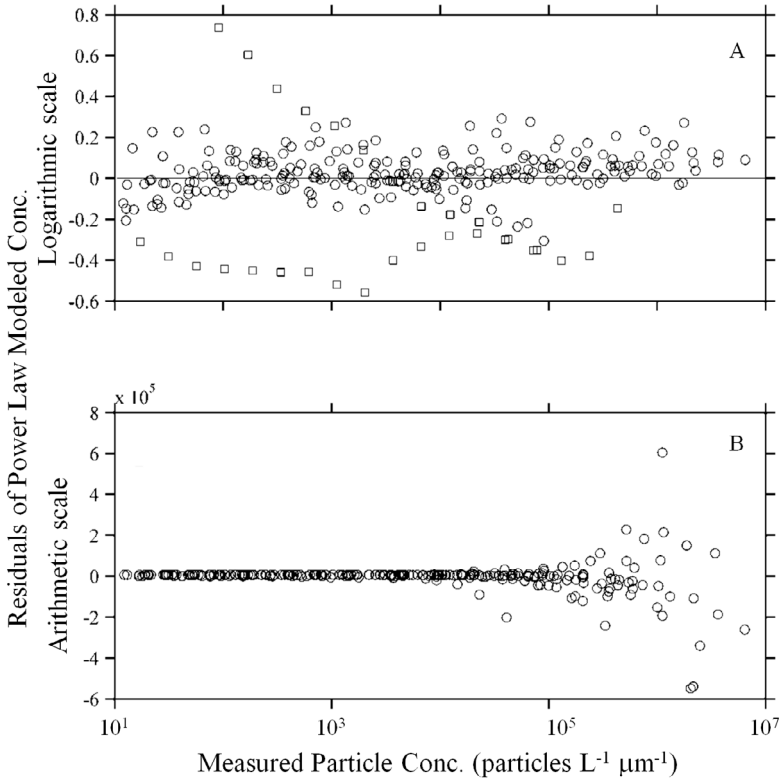

Figure 3. (a) Residuals from a straight line fitted to the log-transformed particle concentration data plotted against the modeled particle concentration for the entire data set (circles). Two cruises (squares), Southern Ocean 2008 and Florida Bay 2005, deviated substantially from the zero line. (b) Residuals from a linear regression on the arithmetic data plotted against the measured particle concentrations.

[19] Evaluating the applicability of the power law using the R^2 value alone, although based on an objective number, is rather subjective in nature. *Gaudoin et al.* [2003] conducted a goodness-of-fit test for the power law process and determined that the critical value at the 5% significance level for a sample size of ~20 (each data set is made up of 22 size classes) was 0.85. According to the study, a measured R^2 less than this threshold would result in a rejection of the null hypothesis that the underlying process follows a power law. All of our 175 stations had values above this threshold, which suggests that these stations follow a power law.

[20] Aggregated statistics were also conducted for each cruise and subregion within each cruise to determine whether the power law fit was generally applicable to various broad categories of seawater (e.g., oceanic, estuarine, river plume). A single regression statistic was calculated for the measured and predicted particle concentrations from all stations within each cruise, subregion, and broader water group. The aggregated statistic showed high R^2 values (>97%) for the broader categories of estuarine, open ocean, and river plume with regression slopes near unity, 0.97–1.02. These high R^2 values and the similarity of the slopes to unity suggests that there was no overall difference in performance of the power law model between the different broad water categories and the first-order approximation of the power law model was generally applicable.

[21] In addition to the regression statistics, we also evaluated the shape of the residuals in order to determine the model fit across the entire size range and any consistent over or under predictions [*Packard and Birchard*, 2008]. The residuals for the logarithmic regression (Figure 3a) generally revealed data clustered around the 0 line with no visible bias. A runs test of the null hypothesis that the residuals come in random order, however, revealed a nonrandom distribution ($p < 0.05$). For two cruises in particular, the Southern Ocean 2008 and Florida Bay 2005 (squares, Figure 3a), the residuals deviated substantially from the zero line. The Southern Ocean waters, in particular, contained significant concentrations of coccolithophores and detached coccoliths and small particle enhancements due to whitecap-induced bubble plumes that contributed to the complexity of the particle assemblages.

[22] A final test of the power law was to consider the data on an arithmetic scale. Even though the particles followed a logarithmic relationship, slopes determined from log-transformed data may no longer be valid when reexpressed on an arithmetic scale due to biasing at one end of a size range [*Packard and Birchard*, 2008]. The modeled particle concentration showed no significant bias with increasing particle counts, particularly at the end of the distribution consisting of high numbers of small particles (Figure 3b). In summary, the power law model proved to be a reasonable approximation for the diversity of oceanic and coastal waters sampled, and the results from the model are further analyzed below.

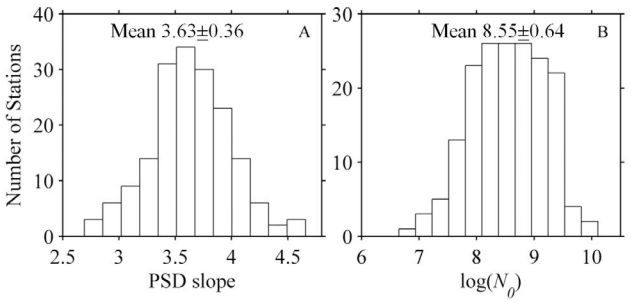

Figure 4. Histograms of the (a) modeled particle size distribution slopes, ξ, and (b) logarithmic concentration factor, N_o, (particles L^{-1} μm^{-1}) at D_0 of 1 μm. Mean and 1 standard deviation are provided for sample size of 175.

3.2. Spatial Variability in Particle Size Distributions

[23] The second objective of this study was to explore regional differences in both relative sizes of particles, expressed as the PSD slope, and concentration (particles L^{-1} μm^{-1}). As noted above, small particles were always more abundant in the water than large particles and the relative abundance of smaller to larger particles increases as the slope of the PSD increases. The PSD slopes from the sampled waters varied from 2.7 to 4.7 (Table 1), covering nearly the entire range observed for natural waters. Measured PSD slopes followed a normal distribution (Jarque-Bera composite normality test, $p = 0.50$) centered on a mean of 3.63 with a 1 standard deviation of 0.36 (n = 175; Figure 4a). The sampled areas spanned virtually every water type, including sloughs with little freshwater input, traditional estuaries, coastal shelves, and the open ocean. The modeled intercept, N_0 (particles L^{-1} μm^{-1}) with D_0 of 1 μm, also followed a lognormal distribution (Jarque-Bera composite normality test, $p = 0.32$) centered at 8.55 with 1 standard deviation of 0.64 (Figure 4b).

[24] PSD from open ocean waters, coastal/estuarine, and river plume waters exhibited distinct distributions (Figure 5). The steepest PSD slopes occurred in the two North Atlantic cruises and the Southern Ocean, indicating a prevalence of smaller particles in these oligotrophic waters. Whereas, the shallowest PSD slopes (slopes of approximately 3) occurred in regions with freshwater inputs, such as the Narragansett Bay and the Connecticut River plume which contain complex particle assemblages (i.e., nonspherical particles, minerogenic and coated particles, etc…), larger particle aggregates, and are typically more productive. We also note that regions with large fluctuations in density such as river plumes (buoyancy frequencies exceeding 0.025 s^{-1}), will be subject to light scattering by schlieren that will falsely indicate accumulations of particles [*Mikkelsen et al.*, 2008]. The relative enhancement of larger particles in the river plume waters, however, may also be associated with aggregates in the low shear zones of the plume [*Ackleson*, 2006]. Low PSD slopes < 3 in Great Florida Bay may be attributed to larger detrital and sand suspensions and potentially the contribution of emergent oxygen bubbles from the productive sea grass beds.

[25] Statistical analyses were performed on the PSD slopes to determine whether the general water types exhibited significantly different PSD slopes and particle concentrations. The sampled regions were roughly divided into those that represented open ocean (North Atlantic, Southern Ocean, and Florida Shelf), estuarine (Elkhorn Slough, St. Joseph Bay, Long Island Sound, and Greater Florida Bay), and river plumes (Connecticut River, Hudson River). The PSD slopes for the open ocean, estuarine, and river plume were found to be significantly different (ANOVA, $p < 0.01$).

[26] Particle concentrations were also highly variable from site to site, ranging from 47 to 10,339 particles L^{-1} μm^{-1} in the 37 μm size class (Table 1). The median particle concentrations were lowest for the open ocean (152 particles L^{-1} μm^{-1}), followed by estuarine (2062 particles L^{-1} μm^{-1}), and then river plume (4319 particles L^{-1} μm^{-1}). Particle concentrations were significantly different for these three water types (ANOVA, $p < 0.01$). The highest particle loads occurred in Raritan Bay, Elkhorn Slough and the river plumes sampled in Long Island Sound. Lowest particle loads occurred in the oligotrophic open ocean stations of the North Atlantic and Southern Ocean.

[27] During March 2007, particle size distributions were measured in the North Atlantic along a transect extending southward from the mouth of Narragansett Bay, across the Gulf Stream to the Sargasso Sea (ENV07, Figure 6). Coincident MODIS Aqua satellite imagery show different levels of phytoplankton biomass (Chl) and sea surface temperature (SST) across this 800 km transect (Figures 6a and 6b). Chlorophyll was high and patchy on the continental shelf (1–4 mg Chl m^{-3}) and then became much lower into the Gulf Stream and further southward (<0.6 mg Chl m^{-3}). SST showed a similar pattern with low temperatures on the shelf and high temperature in the Gulf and Sargasso Sea.

[28] The PSD slope progressed from lower near the coast to higher with distance from the coast (Figure 6c) consistent with a shift toward smaller phytoplankton in the nutrient deplete regions of the Sargasso Sea. Similarly, particle

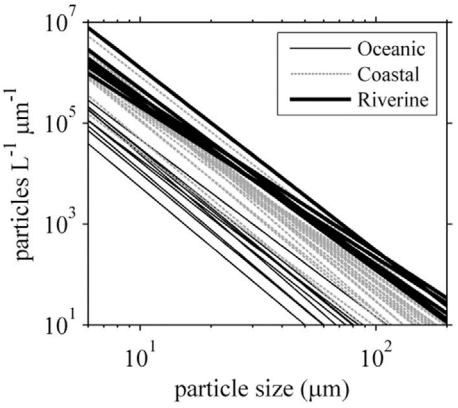

Figure 5. Median particle size distributions calculated for all stations within the cruises identified in Table 1 separated by water type: oceanic, coastal, and riverine. Lines represent the fitted PSD slopes and intercepts. Lower-particle counts and steeper slopes are characteristic of oceanic waters and higher-particle counts and flatter slopes are characteristic of riverine waters.

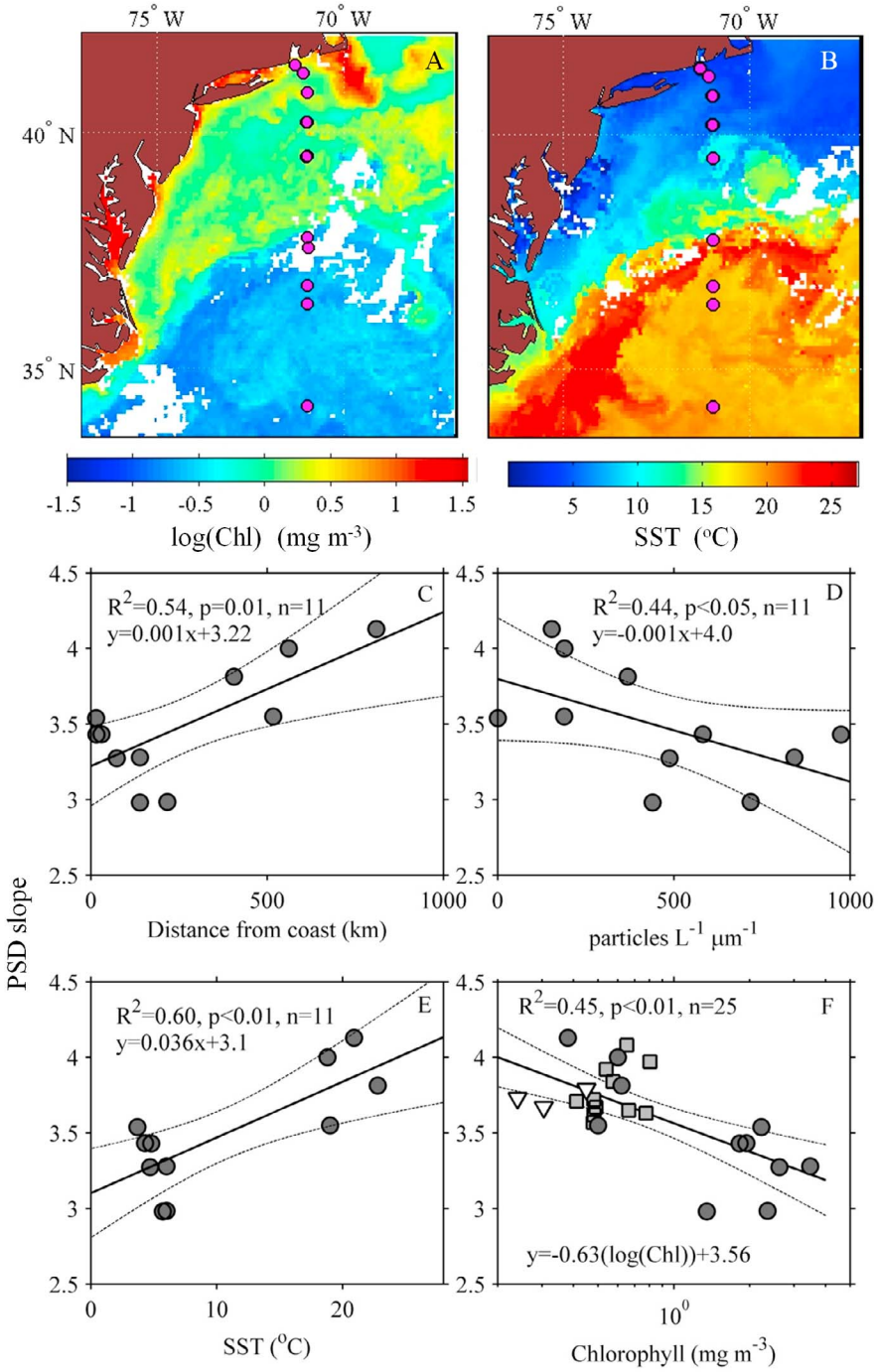

Figure 6. MODIS 8 day time-averaged satellite imagery of the North Atlantic with stations from the *Endeavor* 2007 cruise of (a) chlorophyll *a* (Chl) concentration (mg m^{-3}) and (b) sea surface temperature (°C). Particle slope dynamics from these stations follow the expected biological oceanographic relationships including (c) increasing PSD slope with shortest distance from the coast, (d) decreasing PSD slope with increasing particle concentrations, (e) increasing PSD slope with temperature, and (f) decreasing slope with increasing concentrations of in situ measured Chl from the oceanic stations. Circles represent data from E07, triangles represent data from the Florida shelf, and squares represent data from the Southern Ocean.

concentrations were roughly inversely proportional to the PSD slope with fewer and smaller particles in open ocean conditions and more numerous and larger particles characteristic of the coastal environment (Figure 6d). For SST around 20°C, the PSD slopes averaged 3.7 compared to 3.25 in cold 5°C shelf waters (Figure 6e). These results agree with those of *Sheldon et al.* [1972] who found distinct particle assemblages for the waters in the Gulf Stream and

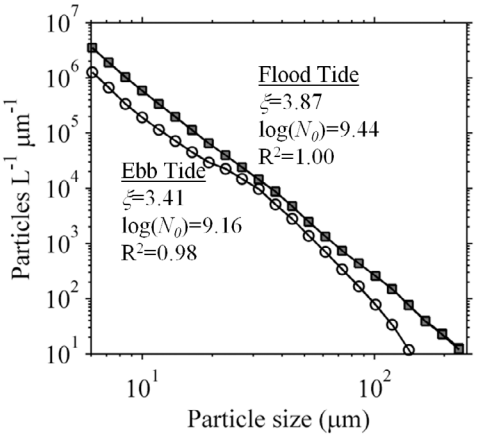

Figure 7. Particle concentrations in Elkhorn Slough, California, showing the increase in particles between two tidal stages, especially in the small- and large-particle size classes. The particle size distribution slope changed greatly between tidal stages, from 3.41 at ebb tide (squares) to 3.87 at high slack tide (circles).

the Sargasso Sea and used this information to map the extent of the Gulf Stream. However, results from the North Atlantic Shelf stations are seasonally dependent varying with the amount of freshwater runoff from the Hudson and Connecticut Rivers. Stations sampled in October 2005 (EDV05) across the shelf showed low particles and higher PSD slopes.

[29] PSD slopes can also be related to biogeochemical properties. Open ocean waters lack significant terrigenous input and the optical properties tend to covary with the concentration of phytoplankton, the so-called bio-optical assumption of Case 1 waters [*Smith and Baker*, 1978]. Since Chl concentrations can be related to phytoplankton size [*Yentsch and Phinney*, 1989; *Chisholm*, 1992; *Loisel et al.*, 2006], we hypothesized that higher Chl would more likely be associated with regions of larger particles (lower PSD slope) and lower Chl with regions of smaller particles (higher PSD slope) [*Sullivan et al.*, 2005]. From the stations sampled in the North Atlantic, a significant inverse relationship was found between measured PSD slopes and Chl (Figure 6f). This relationship described the general decreasing trend in PSD slope with chlorophyll concentrations ranging over an order of magnitude from ~0.2–3 mg Chl m^{-3}.

[30] One anomalous station located on the North Atlantic shelf was excluded from Figure 6 because it contained a surface bloom of small phytoplankton that resulted in an unusually high PSD slope compared to neighboring waters measured at that time. The volumetric PSD for this station indicated a distinct peak at 14 μm size class that was not observed in the neighboring waters, even though the station still followed a power law distribution ($R^2 = 0.98$; $p < 0.01$; PSD slope = 4.61; $\log(N_0) = 9.53$ particles L^{-1} μm^{-1}; Chl = 6.5 mg m^{-3}). Consistent with nutrient regimes in the open ocean [*Yentsch and Phinney*, 1989], however, the majority of open ocean stations support the general trend that higher Chl conditions are related to larger phytoplankton and lower Chl with smaller phytoplankton. Such relationships have relevance to understanding the role of phytoplankton in ecosystem structure, carbon export, and the larger climate cycle.

3.3. Temporal Variability in Particle Size Distributions

[31] While the above analysis demonstrated the large-scale spatial trends in the PSD, environmental forces, such as storm events and the regular periodicity of tides, can cause high levels of temporal variability within a locale. Recent storm activity, for example, can dramatically alter sediment loads in a water column. Hurricanes Edouard and Hortense introduced enough energy into a 70 m deep water column to resuspend bottom sediments over 30 m above the bottom [*Chang et al.*, 2001]. Even lower but persistent winds can cause shallow water Langmuir "Supercells" that can serve to redistribute benthic algae and resuspend sediments off the seafloor [*Gargett et al.*, 2004; *Dierssen et al.*, 2009a, 2009b]. Once suspended, sediments can persist in the water column for several days. Sampling in St. Joseph Bay, FL (PSJ06) took place immediately following Tropical Storm Alberto in June 2006. This bay had dense seagrass beds ringing the shores (<2 m) that transitioned to deeper water (~10 m) toward the middle of the bay. Normal tidal flow in such a bay would not be sufficient to resuspend sediment beyond a few meters above the seafloor [*Fugate and Friedrichs*, 2002]. However, after the passage of Tropical Storm Alberto, the water appeared of a brownish color due to the high sediment load [*Dierssen et al.*, 2006] and the median particle concentration was high throughout the shallow and deep portions of the Bay (1740 and 2143 particles L^{-1} μm^{-1}, respectively). Moreover, the PSD slopes were not significantly different between the shallow and deep stations (Mean 3.41 and 3.51, respectively).

[32] A strong tide can also significantly modify the particle size distribution of the water column, especially in shallow water. In 1947, the Army Corps of Engineers breached the shoreline dunes and dredged a wide, deep channel to permit entry of boats into the newly created Moss Landing Harbor thereby altering the sluggish tidal character of the Elkhorn Slough embayment. Following the opening of the new mouth, an unprecedented volume of tidal flow inundated the wetlands and, in the last 20 years, current speeds near the mouth have doubled and tidal volume increased by 43% [*Wasson et al.*, 2001]. Today, the tidal range varies over 2 m in amplitude and significantly alters the particle dynamics. The water of Elkhorn Slough was brown in color [*Dierssen et al.*, 2006] and had one of the highest particle concentrations of any water type sampled in this study. Measurements along the shore of Elkhorn Slough at two tidal stages resulted in markedly different particle loads and PSD slopes (Figure 7). The station sampled from ebb tide had relatively larger particles (PSD slope 3.4) compared to that sampled during high slack tide (PSD slope 3.8). In regions with high tidal scour, such as Elkhorn Slough, an understanding of the particle dynamics will be closely linked to the tidal phase and must be considered when assessing sediment fluxes in these regions.

[33] Tidal currents may also impact coastal particle dynamics differently depending on the benthic composition. Dense sea grass beds can reduce currents inside the beds by a factor of 2 to 10 [*Gambi et al.*, 1990] and the magnitude of

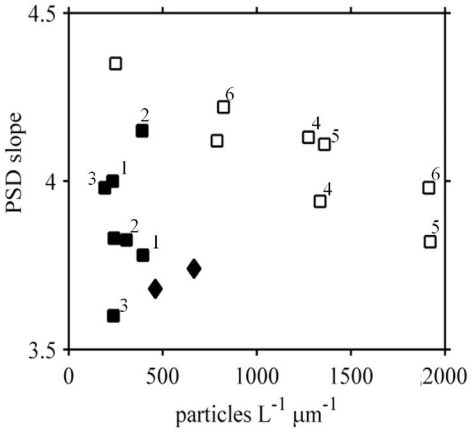

Figure 8. Particle concentration at the 37 μm particle size versus the particle size distribution slope for the FBOP 2006 cruise to Florida Bay by subregion showing the disparate trends for low-density (open squares) and high-density sea grass (solid squares) and algal film stations (diamonds). The numbered points are the same location sampled on different days within a 2 week period.

this current reduction depends on the shoot density of the seagrass bed [*Koch*, 2001]. These factors may result in differences in particle size distributions measured in waters overlying sea grass beds and sand flats, respectively. The same location sampled at different tidal stages in Florida Bay 2006, for example, revealed different particle dynamics (Figure 8). However, the tidal variability was less than the influence of benthic type on particle dynamics. In low shoot density areas (<300 shoots/m^2), higher particle loads were coupled with shallower PSD slopes. In contrast, stations with high shoot density (>1000 shoots/m^2) had considerably lower particle loads in the overlying water column, yet varying PSD slopes sampled over time. These two benthic types were statistically different in both particle load and PSD slope (ANOVA, $p < 0.01$). Consistent with the results of *Koch* [2001], dense seagrass beds were found to reduce sediment resuspension within the bed and the particle concentrations were low. However, particles suspended within overlying water were largely uncoupled from sediment within the bed and the PSD slopes were more dependent on the tidal cycle rather than the benthic composition. Gaps in low-density sea grass beds can allow faster currents to enter the bed and resuspend sediments of all sizes, lowering the PSD slope [*Granata et al.*, 2001].

[34] Further confirmation of this mechanism was evident in two stations with sparse sea grass concentrations (364 and 451 shoots/m^2), but considerable biofilm on the sediments. Biofilms are coatings on the surfaces of sediment particles consisting of photosynthetic and nonphotosynthetic microbial cells embedded within a secreted matrix of extracellular polymers [*Costerton et al.*, 1995]. Biofilms cannot only influence the color and reflectance of the sediment [*Decho et al.*, 2003], but similar to dense sea grass beds, can also serve to limit sediment resuspension from the seabed. As shown in Figure 8 (diamonds), the water overlying the two biofilm stations did not have high particle loads like the other sparse seagrass stations, but rather had low particle concentrations similar to the dense seagrass beds. These results show how tides and benthic composition together can influence the PSD slope and illustrate the large variability in localized particle composition and abundance in coastal embayments and estuaries prone to sediment resuspension.

[35] Further studies should extrapolate this analysis to smaller particles, particularly those in micron and submicron-size classes. Some have suggested that smaller particles < 5μm in productive natural waters do not follow a power law distribution [*Kitchen et al.*, 1982]. However, particles with a diameter 0.6–1 μm sampled from the Southern Pacific were fit with a power law and found to have a much higher PSD slope (~6) than those from 1 to 17 μm [*Risovic*, 1993; *Loisel et al.*, 2006]. Moreover, coupling these results with additional measurements of physical parameters (e.g., current and turbulence data), optical parameters (e.g., volume scattering function, backscattering ratio), estimates of total suspended loads, and phytoplankton functional groups may lead to further insights into the dynamics of both coastal and open ocean ecosystems and further parameterize marine contributions to the carbon cycle. Higher temporal resolution measurements may also reveal other types of variability, such as diel periodicity in cell size associated with growth rates [*Sosik et al.*, 2003].

4. Conclusions

[36] The power law approximation proved an effective model of the natural particle size distribution over the measured size range for all of the water types sampled (6–250 μm). The 175 stations had high R^2 values and could be well described by a power law approximation and the back-calculated regression slopes and intercepts approached their ideal values of 1.0 and 0, respectively. This confirms the power law approximation as a valid method for parameterizing the particle size distribution across a wide variety of water types for particles in this size range, including complex coastal regions and embayments. The measured PSD slopes derived from the power law approximation ranged from 2.7 to 4.7, were normally distributed about a mean of 3.6 and were consistent with the general patterns expected for river plume, estuarine, and oligotrophic waters. The surface waters of the open ocean had the fewest suspended particles and the steepest slopes, the estuarine waters had higher particle loads and less steep slopes, and the river plume stations had the highest particle loads and the flattest slopes indicating a relative prevalence of larger particles. A relationship was found in the oligotrophic waters of the North Atlantic associating higher slopes with low chlorophyll concentrations and lower slopes with higher chlorophyll concentrations.

[37] Changes in PSD slopes and particle concentrations were also observed temporally in areas experiencing storm activity and strong tidal mixing. In shallow water, such influences are largely dependent upon the composition of the seafloor. Seagrass beds are particularly resilient to large storm activity [*Dierssen et al.*, 2003] and serve to decrease sediment resuspension compared to sand-covered regions. However, the PSD slope was found to vary considerably among these stations and within a single station over time, presumably due to different stages of the tidal cycle that influence the particle assemblages.

[38] **Acknowledgments.** This work was funded by the Office of Naval Research Optics Program (H. M. Dierssen) and National Aeronautic and Space Administration's Ocean Biology and Biogeochemistry research program (H.M. Dierssen). Many thanks to the Long Island Sound Integrated Coastal Observation System (LISICOS); the crew aboard the R/V *Connecticut*, R/V *Endeavor*, and R/V *Ronald Brown*; the State of Rhode Island for R/V *Endeavor* ship time; Steve Ackleson for ship time on the R/V *Connecticut*; the staff at Moss Landing Marine Laboratories, Keys Marine Laboratory, and St. Joseph Bay Preserves Center; Hans Dam and James Edson for scientific input and editorial support; and University of Connecticut's Marine Science and Technology Center and Jeff Godfrey for diving support.

References

Ackleson, S. (2006), Optical determinations of suspended sediment dynamics in western Long Island Sound and the Connecticut River plume, *J. Geophys. Res.*, *111*, C07009, doi:10.1029/2005JC003214.

Agrawal, Y., and H. Pottsmith (2000), Instruments for particle size and settling velocity observation in sediment transport, *Mar. Geol.*, *168*, 89–114, doi:10.1016/S0025-3227(00)00044-X.

Agrawal, Y., and P. Traykovski (2001), Particles in the bottom boundary layer: Concentration and size dynamics through events, *J. Geophys. Res.*, *106*(C5), 9533–9542, doi:10.1029/2000JC900160.

Agrawal, Y., A. Whitmire, O. Mikkelsen, and H. Pottsmith (2008), Light scattering by random shaped particles and consequences on measuring suspended sediments by laser diffraction, *J. Geophys. Res.*, *113*, C04023, doi:10.1029/2007JC004403.

Anglès, A., A. Jordi, E. Garcés, M. Masó, and G. Basterretxea (2008), High-resolution spatio-temporal distribution of a coastal phytoplankton bloom using laser in situ scattering and transmissometry (LISST), *Harmful Algae*, *7*, 808–816, doi:10.1016/j.hal.2008.04.004.

Aurin, D., H. M. Dierssen, M. S. Twardowski, and C. S. Roesler (2010), Optical complexity in Long Island Sound and implications for coastal ocean color remote sensing, *J. Geophys. Res.*, *115*, C07011, doi:10.1029/2009JC005837.

Bader, H. (1970), The hyperbolic distribution of particle sizes, *J. Geophys. Res.*, *75*(15), 2822–2830, doi:10.1029/JC075i015p02822.

Boss, E., M. Twardowski, and S. Herring (2001), Shape of particulate beam attenuation spectrum and its inversion to obtain the shape of the particle size distribution, *Appl. Opt.*, *40*(27), 4885–4893, doi:10.1364/AO.40.004885.

Briucaud, A., A. Morel, and L. Prieur (1981), Absorption by dissolved organic matter of the sea (yellow substance) in the UV and visible domains, *Limnol. Oceanogr.*, *26*, 43–53, doi:10.4319/lo.1981.26.1.0043.

Buonassissi, C. J. (2009), A regional comparison of particle size distributions and the power-law approximation in oceanic and estuarine surface waters by laser diffraction, M.S. thesis, *Dep. of Mar. Sci.*, Univ. of Conn., Groton, Conn.

Carder, K., G. Beardsley Jr., and H. Pak (1971), Particle size distributions in the eastern equatorial Pacific, *J. Geophys. Res.*, *76*(21), 5070–5077, doi:10.1029/JC076i021p05070.

Chang, G., T. Dickey, and A. Williams III (2001), Sediment resuspension over a continental shelf during Hurricanes Edouard and Hortense, *J. Geophys. Res.*, *106*(C5), 9517–9531, doi:10.1029/2000JC900032.

Chisholm, S. W. (1992), Phytoplankton size, in Primary Productivity and Biogeochemical Cycles in the Sea, edited by P. G. Falkowski and A. D. Woodhead, pp. 213–237, Plenum, New York.

Costerton, J. W., Z. Lewandowski, D. E. Caldwell, D. R. Korber, and H. M. Lappin-Scott (1995), Microbial biofilms, *Annu. Rev. Microbiol.*, *49*, 711–745.

Decho, A., T. Kawaguchi, M. Allison, E. Louchard, R. Reid, F. Stephens, K. Voss, R. Wheatcroft, and B. Taylor (2003), Sediment properties influencing upwelling spectral reflectance signatures: The "biofilm gel effect," *Limnol. Oceanogr.*, *48*, 431–443, doi:10.4319/lo.2003.48.1_part_2.0431.

Dierssen, H. M., R. C. Zimmerman, R. A. Leather, T. V. Downes, and C. O. Davis (2003), Ocean color remote sensing of seagrass and bathymetry in the Bahamas Banks by high resolution airborne imagery, *Limnol. Oceanogr.*, *48*, 444–455, doi:10.4319/lo.2003.48.1_part_2.0444.

Dierssen, H. M., R. M. Kudela, J. P. Ryan, and R. C. Zimmerman (2006), Red and black tides: Quantitative analysis of water-leaving radiance and perceived color for phytoplankton, colored dissolved organic matter, and suspended sediments, *Limnol. Oceanogr.*, *51*, 2646–2659, doi:10.4319/lo.2006.51.6.2646.

Dierssen, H. M., R. C. Zimmerman, and D. J. Burdige (2009a), Optics and remote sensing of Bahamian carbonate sediment whitings and potential relationship to wind-driven Langmuir circulation, *Biogeosciences*, *6*(3), 487–500, doi:10.5194/bg-6-487-2009.

Dierssen, H. M., R. C. Zimmerman, L. A. Drake, and D. J. Burdige (2009b), Potential export of unattached benthic macroalgae to the deep sea through wind-driven Langmuir circulation, *Geophys. Res. Lett.*, *36*, L04602, doi:10.1029/2008GL036188.

Falkowski, P. G., R. T. Barber, and V. Smetacek (1998), Biogeochemical controls and feedbacks on ocean primary production, *Science*, *281*, 200–206, doi:10.1126/science.281.5374.200.

Fugate, D., and C. Friedrichs (2002), Determining concentration and fall velocity of estuarine particle populations using ADV, OBS and LISST, *Cont. Shelf Res.*, *22*, 1867–1886, doi:10.1016/S0278-4343(02)00043-2.

Gambi, M., A. Nowell, and P. Jumars (1990), Flume observations on flow dynamics in *Zostera marina* (eelgrass) beds, *Mar. Ecol. Prog. Ser.*, *61*, 159–169, doi:10.3354/meps061159.

Gargett, A., J. Wells, A. Tejada-Martinez, and C. Grosch (2004), Langmuir supercells: A mechanism for sediment resuspension and transport in shallow seas, *Science*, *306*, 1925–1928, doi:10.1126/science.1100849.

Gaudoin, O., B. Yang, and M. Xie (2003), A simple goodness-of-fit test for the power-law process, based on the Duane plot, *IEEE Trans. Reliab.*, *52*, 69–74, doi:10.1109/TR.2002.805784.

Granata, T., T. Serra, J. Colomer, X. Casamitjana, C. Duarte, and E. Gacia (2001), Flow and particle distribution in a nearshore meadow before and after a storm, *Mar. Ecol. Prog. Ser.*, *218*, 96–106.

Holm-Hansen, O., C. Lorenzen, R. Holmes, and J. Strickland (1965), Fluorometric determination of chlorophyll, *ICES J. Mar. Sci.*, *30*(1), 3–15, doi:10.1093/icesjms/30.1.3.

Jackson, G., D. Maffione, A. Costello, B. Alldredge, B. Logan, and H. Dam (1997), Particle size spectra between 1um and 1 cm at Monterey Bay determined using multiple instruments, *Deep Sea Res. Part I*, *44*, 1739–1767, doi:10.1016/S0967-0637(97)00029-0.

Jonasz, M. (1983), Particle size distribution in the Baltic, *Tellus B*, *35*, 346–358, doi:10.1111/j.1600-0889.1983.tb00039.x.

Jonasz, M., and G. Fournier (1996), Approximation of the size distribution of marine particles by a sum of log-normal functions, *Limnol. Oceanogr.*, *41*, 744–754, doi:10.4319/lo.1996.41.4.0744.

Jonasz, M., and G. Fournier (2007), Light Scattering by Particles in Water: Theoretical and Experimental Foundations, Academic, London.

Junge, C. (1963), *Chemistry and Radioactivity*, Academic, London.

Karp-Boss, L., L. Azevedo, and E. Boss (2007), LISST-100 measurements of phytoplankton size distribution: Evaluation of the effects of cell shape, *Limnol. Oceanogr. Methods*, *5*, 396–406.

Kitchen, J. (1977), Particle size distributions and the vertical distribution of suspended matter in the upwelling region off Oregon, Ph.D. dissertation, Oreg. State Univ., Corvallis, Oreg.

Kitchen, J., D. Menzies, H. Pak, and J. Zaneveld (1975), Particle size distributions in a region of coastal upwelling analyzed by characteristic vectors, *Limnol. Oceanogr.*, *20*, 775–783, doi:10.4319/lo.1975.20.5.0775.

Kitchen, J., J. R. V. Zaneveld, and H. Pak (1982), Effect of particle size distribution and chlorophyll content on beam attenuation spectra, *Appl. Opt.*, *21*(21), 3913–3918, doi:10.1364/AO.21.003913.

Koch, E. (2001), Beyond light: Physical, geological and geochemical parameters as possible submersed aquatic vegetations habitat requirements, *Estuaries*, *24*, 1–17, doi:10.2307/1352808.

Kostadinov, T., D. A. Siegel, and S. Maritorena (2009), Retrieval of the particle size distribution from satellite ocean color observations, *J. Geophys. Res.*, *114*, C09015, doi:10.1029/2009JC005303.

Le Quéré, C., et al. (2005), Ecosystem dynamics based on plankton functional types for global ocean biogeochemistry models, *Global Change Biol.*, *11*, 2016–2040.

Loisel, H., J. M. Nicolas, A. Sciandra, D. Stramski, and A. Poteau (2006), Spectral dependency of optical backscattering by marine particles from satellite remote sensing of the global ocean, *J. Geophys. Res.*, *111*, C09024, doi:10.1029/2005JC003367.

Middleton, G., and J. Southard (1984), *Mechanics of Sediment Movement*, *SEPM Short Courses Notes Ser.*, vol. 3, Soc. for Sediment. Geol., Tulsa, Okla.

Mikkelsen, O., and M. Pejrup (2001), The use of a LISST-100 laser particle sizer for in-situ estimates of floc size, density and settling velocity, *Geo Mar. Lett.*, *20*, 187–195, doi:10.1007/s003670100064.

Mikkelsen, O. A., T. J. Milligan, P. S. Hill, R. Chant, C. F. Jago, S. E. Jones, V. Krivtsov, and G. Mitchelson-Jacob (2008), The influence of schlieren on in situ optical measurements used for particle characterization, *Limnol. Oceanogr. Methods*, *6*, 133–143.

Monahan, E. C., and C. R. Zietlow (1969), Laboratory comparisons of fresh-water and salt-water whitecaps, *J. Geophys. Res.*, *74*(28), 6961–6966, doi:10.1029/JC074i028p06961.

Packard, G., and G. Birchard (2008), Traditional allometric analysis fails to provide a valid predictive model for mammalian metabolic rates, *J. Exp. Biol.*, *211*, 3581–3587, doi:10.1242/jeb.023317.

Pedocchi, F., and M. H. Garcia (2006), Evaluation of the LISST-ST instrument for suspended particle size distribution and settling velocity measurements, *Cont. Shelf Res.*, *26*, 943–958, doi:10.1016/j.csr.2006.03.006.

Risovic, D. (1993), Two-component model of sea particle size distribution, *Deep Sea Res. Part I*, *40*, 1459–1473, doi:10.1016/0967-0637(93)90123-K.

Seibel, B. A. (2007), On the depth and scale of metabolic rate variation: Scaling of oxygen consumption rates and enzymatic activity in the class *cephalopoda* (*Mollusca*), *J. Exp. Biol.*, *210*, 1–11, doi:10.1242/jeb.02588.

Sheldon, R., A. Prakash, and W. Sutcliffe Jr. (1972), The size distribution parameters of particles in the ocean, *Limnol. Oceanogr.*, *17*, 327–340, doi:10.4319/lo.1972.17.3.0327.

Shifrin, K., and G. Tonna (1993), Inverse problem related to light scattering in the atmosphere and ocean, *Adv. Geophys.*, *34*, 175–252.

Slade, W., and E. Boss (2006), Calibrated near-forward volume scattering function obtained from the LISST particle sizer, *Opt. Express*, *14*(8), 3602–3615, doi:10.1364/OE.14.003602.

Smith, R., and K. Baker (1978), The bio-optical state of ocean waters and remote sensing, *Limnol. Oceanogr.*, *23*, 247–259, doi:10.4319/lo.1978.23.2.0247.

Sosik, H. M., R. J. Olson, M. G. Neubert, A. Shalapyonok, and A. R. Solow (2003), Growth rates of coastal phytoplankton from time-series measurements with a submersible flow cytometer, *Limnol. Oceanogr.*, *48*, 1756–1765, doi:10.4319/lo.2003.48.5.1756.

Stavn, R., and T. Keen (2004), Suspended minerogenic particle distributions in high-energy coastal environments: Optical implications, *J. Geophys. Res.*, *109*, C05005, doi:10.1029/2003JC002098.

Stramski, D., and D. Kiefer (1991), Light scattering by microorganisms in the open ocean, *Prog. Oceanogr.*, *28*, 343–383, doi:10.1016/0079-6611(91)90032-H.

Sullivan, J., M. Twardowski, P. Donaghay, and S. Freeman (2005), Use of optical scattering to discriminate particle types in coastal waters, *Appl. Opt.*, *44*(9), 1667–1680, doi:10.1364/AO.44.001667.

Twardowski, M., E. Boss, J. MacDonald, S. Pegau, A. Barnard, and J. Zaneveld (2001), A model for estimating bulk refractive index from the optical backscattering ratio and the implications for understanding particle composition in case I and case II waters, *J. Geophys. Res.*, *106*(C7), 14,129–14,142, doi:10.1029/2000JC000404.

van de Hulst, H. C. (1981), Light Scattering by Small Particles, 470 pp., Dover, Mineola, N. Y.

Vidondo, B., Y. T. Prairiej, M. Blanco, and C. M. Duarte (1997), Some aspects of the analysis of size spectra in aquatic ecology, *Limnol. Oceanogr.*, *42*, 184–192, doi:10.4319/lo.1997.42.1.0184.

Wasson, K., E. Van Dyke, R. Kvitek, J. Brantner, and S. Bane (2001), Tidal erosion at Elkhorn Slough, report, Elkhorn Slough Found., Moss Landing, Calif. (Available at http://www.elkhornslough.org/research/PDF/tidal_erosion_ES.pdf.)

Yentsch, C. S., and D. A. Phinney (1989), A bridge between ocean optics and microbial ecology, *Limnol. Oceanogr.*, *34*, 1694–1705, doi:10.4319/lo.1989.34.8.1694.

C. J. Buonassissi, Institute for Coastal Science and Policy, East Carolina University, Flanagan Suite 250, Greenville, NC 27858, USA.

H. M. Dierssen, Department of Marine Sciences, University of Connecticut, Groton, CT 06340, USA. (heidi.dierssen@uconn.edu)